Quantum gates by coupled asymmetric quantum dots and controlled-NOT-gate operation

Tetsufumi Tanamoto
Corporate Research and Development Center, Toshiba Corporation, Saiwai-ku, Kawasaki 210-8582, Japan
(Received 2 March 1999; published 12 January 2000)

A quantum computer based on an asymmetric coupled-dot system has been proposed and shown to operate as a controlled-NOT gate. The basic ideas are the following. (1) The electron is localized in one of the asymmetric coupled dots. (2) The electron transfer takes place from one dot to the other when the energy levels of the coupled dots are set to be close. (3) The Coulomb interaction between the coupled dots mutually affects the energy levels of the other coupled dots. The decoherence time of the quantum computation and the measurement time are estimated. The proposed system can be realized by developing the technology of the single-electron memory using Si nanocrystals, and a direct combination of the quantum circuit and the conventional circuit is possible.

PACS number(s): 03.67.Lx, 03.65.−w, 73.23.−b

I. INTRODUCTION

Since Shor's factorization program was proposed, many studies have been carried out with a view to realizing the quantum computer [1–7]. Although coherence is necessary for a quantum calculation, it is considered to be difficult to maintain coherence in the entire calculation process throughout the entire circuit. Thus it will be more efficient and more realistic to combine the quantum computational circuit and the conventional LSI circuit in the same chip. Some proposals regarding the quantum computer based on semiconductor physics have been made from this viewpoint [3–5].

Kane [5] proposed a Si-based quantum computer using NMR of dopants (phosphorus). This idea is very promising because the qubits are isolated from the external environment, which causes decoherence. However, controlling the implantation of phosphorus exactly into the definite positions of the Si substrate will depend on future technology, and the usage of the magnetic field seems to be undesirable in the conventional Si LSI circuit. Here we propose a coupled-quantum-dot quantum computer, which can be operated only by electrical effects and show that it can operate as a controlled-NOT gate. It is shown to be realized by developing the technology of a single-electron memory of Si nanocrystals [8,9].

The controlled-NOT operation is given by [3] $|\epsilon_1\rangle|\epsilon_2\rangle \rightarrow |\epsilon_1\rangle|\epsilon_1 \oplus \epsilon_2\rangle$(modulo2) where ϵ_1 shows a *control qubit* and ϵ_2 shows a *target qubit*. The value of ϵ_1 remains unchanged, whereas that of ϵ_2 is changed only if $\epsilon_1 = 1$. This operation is important because it acts as a measurement gate, and produces the entanglement [3] which plays an important role in quantum cryptography gates [10]. In this paper we show the quantum gates of the semiconductor coupled quantum dots, emphasizing their controlled-NOT operation.

The structure of the paper is as follows. In Sec. II the basic idea of this paper is presented, and the static and dynamic properties of the coupled quantum dots operating as a quantum gate are discussed. In Sec. III we estimate the decoherence time in the quantum operation and the measurement time in the detection process of the proposed coupled-quantum-dot system. We also discuss the fabrication process of the coupled-quantum-dot system. Conclusions are presented in Sec. IV.

II. CONTROLLED-NOT GATE BY THE TWO COUPLED DOTS

Coupled-quantum-dot systems with a few electrons have been extensively investigated in regard to many-body effects such as the Coulomb blockade [11–16]. From experiments by van der Vaart *et al.* [13], it can be seen that the electron transfer between dots occurs when the discrete energy level of one of the dots matches that of the other dot of the coupled dots. Pfannkuche and Ulloa [14] showed theoretically that, as a result of the correlations between a few electrons in quantum dots, the electrons behave as if they were noninteracting electrons. Crouch *et al.* [15] and Waugh *et al.* [16] showed that, if the tunneling barrier is low and the coupling of the two dots is strong, the coupled dots behave as a large single dot in a Coulomb blockade phenomenon. This means that, if the tunneling barrier between the dots is sufficiently small, it is possible that only one electron exists in the coupled dots.

Thus, we can consider the electronic state of the two coupled dots in the range of the free-electron approximation [17,18] at the first step of investigation. When two dots of different size are coupled and one excess electron is inserted, the system can be treated as a two-state system where the energy levels of the total coupled-dot system show the localized state of the wave function reflecting the different energy levels of the independent isolated dots [17]. When gate bias voltage is applied and the potential slope is changed, there appears a gate bias voltage $V_{\rm res}$ at which the two energy levels of the original single dots coincide, and the electron transfers to another dot (resonant tunneling). Coupling removes the degeneracy of energy levels in the single-dot quantum states, and produces new states of delocalization such that the even- and odd-parity wave functions spread over the two coupled dots. Thus if we regard the perfect localization of the charge in one of the coupled dots as the ''$|1\rangle$'' state and that in the other dot as the ''$|0\rangle$'' state, we can constitute a *qubit* by the coupled quantum dots (Fig. 1).

The point is, by adjusting the gate bias, we can control the

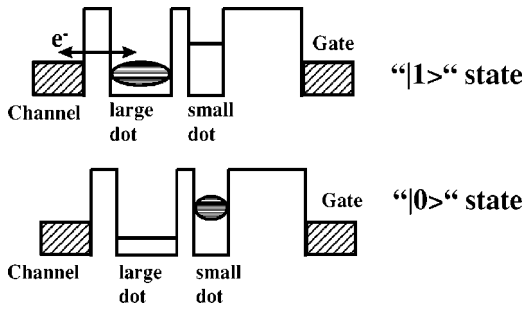

FIG. 1. Coupled quantum dot as a qubit: a large quantum dot and a small quantum dot are coupled such that the larger dot is set close to the channel from which one excess electron is inserted into the coupled dots. The smaller dot is set near the gate electrode via a thick tunnel barrier which controls the energy levels of the coupled dots. A localized electron in the larger dot expresses the $|1\rangle$ state and that in the smaller dot expresses the $|0\rangle$ state.

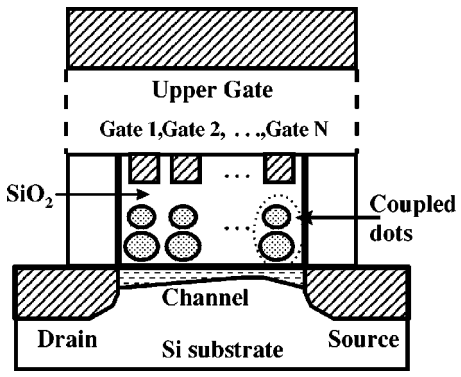

FIG. 3. An example of the N coupled-dot system of quantum computing. Dots are coupled in the longitudinal direction. The electron transfer in the lateral direction is assumed to be neglected. The FET channel structure enables the detection of a small signal of the charge distribution in coupled quantum dots.

electronic state from the localized regions ($|1\rangle$ and $|0\rangle$) to the intermediate delocalized region only where the electron transfers from one dot to the other in the coupled dots in a short time ($\sim$1 ps) [17,18]. As the tunneling barrier structure is asymmetric, the leak current through the coupled-dot system is extremely small [19] and actually neglected.

When the above coupled dots (qubits) are arrayed side by side, the charge distribution of the electron in a qubit changes the potential profiles and the energy levels of the neighboring qubits by its electric field. We assume that the electron transfer between different qubits can be neglected. Then the electronic state in a qubit is affected by whether the electrons in other qubits stay in the $|1\rangle$, on $|0\rangle$ state, or in an arbitrary superposition state of $|1\rangle$ and $|0\rangle$. By changing the charge distribution of the array of qubits, we can operate the total charge distribution of the electrons and the quantum circuit. Figure 2 shows the case of the two-qubit controlled-NOT gate, where one set of the coupled dots operates as a *control qubit* and the other as a *target qubit*. Below, it is shown numerically that this array of the coupled quantum dot operates as the controlled-NOT gate.

One of the candidates for the coupled dots of the quantum computer is considered to be the Si nanocrystals embedded in the gate insulator (Fig. 3). This is based on Si LSI technology similar to that of Tiwari and co-workers single-electron memory [8] (see also Ref. [9]), which is extensively investigated because it operates at room temperature. The

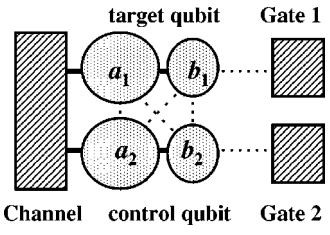

FIG. 2. Quantum gates (controlled-NOT gate) are constituted by setting the coupled dots of Fig. 1 close to each other with a common channel. Solid lines show the path of electron tunneling. Dotted lines show the electric fields generated between quantum dots, or between quantum dots and gates.

excess charge is supplied from the inversion layer in the substrate. By setting larger dots near the channel, the structure shown in Fig. 2 can be realized. The arrangement of the gate electrodes which control the individual qubits depends on the individual algorithm. The simplest form is the case where there are two gate electrodes and two sets of coupled dots (Fig. 2), which works as the controlled-NOT gate explained in this paper. The *measurements* process is operated by the upper gate electrode which controls the overall channel carrier density. The upper gate also protects the electronic states in the dots from disturbance by shielding the external electromagnetic field. The qubits interact mutually and the distribution of the charges affects the current flow (channel conductance) between the source and drain and the threshold gate voltage. A $|11\rangle$ state shifts the threshold voltage most, and a $|00\rangle$ state shifts it least. Because of the sloping channel depth from the source to the drain, the $|10\rangle$ and $|01\rangle$ states can be distinguished. Thus the quantum-mechanical calculation proceeds as follows: (1) To *initialize* the charge distribution (initial quantum states), a large voltage is applied on the upper gate over the coupled dots, and unifies the charge distribution in the coupled dots. (2) The input and output signals are added through the gates over each qubit. (3) The final distribution of charges (final quantum states) is detected by the current between the source and drain and the threshold voltage shifts of the upper gates over the coupled dot system.

When there are many qubits, the controlled-NOT operation of pairs of qubits is affected by the quantum states of the surrounding qubits. That is, the applied gate voltage of operation changes depending on the quantum states of other qubits. This is the same situation as the qubits of Barenco *et al.* [3]. Although the decoupling schemes used in NMR experiments can be applied to avoid the coupling between qubits, it is considered to be desirable that the general quantum calculations are designed by considering the arrangement of qubits [20]. This structure of the proposed system has the merit that the charge distribution in the coupled-dot system, which is considered to be a very small signal, is expected to be detected by the channel conductance with high sensitivity like that of the single-electron memory [8]. Similar to Tiwari

et al.'s single-electron memory, the charging effect appears between the coupled dots and the channel region, and the probability that two electrons come into the qubits is very small as long as the capacitance of the junction is sufficiently small.

In principle, qubits due to semiconductor quantum dots with discrete energy levels do not directly require that the quantum dots be asymmetric. Two coupled quantum dots with discrete energy levels can organize the two-state system. However, when the coupled dots are embedded in the field-effect-transistor (FET)-insulating layer that we propose, the asymmetry of the coupled dots is required for the following two reasons. First, in order to prevent the electron in the coupled dots from returning to channel region in the substrate during the quantum operation, a finite voltage is required. The second reason is related to the measurement process. For the current to flow, a finite gate voltage that is larger than the threshold voltage is required. Because, as discussed below, a large gate voltage breaks the coherent state of the coupled dots, much voltage cannot be applied on the gate electrode. Thus it is desirable that the two discrete energy levels of the quantum dots coincide under the applied gate voltage, and the quantum calculation and the measurement be carried out near the threshold gate voltage. These are the reasons why the asymmetry of the coupled quantum dots is required.

Below, we show the static properties of the wave function of the localized electron by using the *S*-matrix theory and the controlled-NOT operation of the coupled dots. The periodical motion of the localized electron is shown by solving a time-dependent Schrödinger equation. The exact theoretical treatment of the coupled-dot system would be to solve the exact three-dimensional Schrödinger equation. However, since this direct method is difficult to apply in practice, we use the following approximations. The static behavior is studied by solving the one-dimensional Schrödinger equation, and the dynamic behavior, which is more difficult to treat, is studied by regarding the quantum dots as zero-dimensional objects.

A. Static properties of the qubit of the coupled quantum dots

The static properties of the wave function in the coupled dots can be shown by applying the *S*-matrix theory [21] to the one-dimensional case. The one-dimensional Schrödinger equation is given by

$$\left[-\frac{\hbar^2}{2m_i}\frac{\partial^2}{\partial z^2}+V_i(z)\right]\psi_i(z)=E\psi_i(z), \tag{1}$$

where $i(=1,\ldots,N_m)$ show the number of the mesh in the calculation. It is well known that a relatively small number of N_m is sufficient for the calculation (here $N_m\sim 1000$). The electric fields by other coupled dots are considered to be included in the potential, $V_i(z)$. We use the plane-wave approximation for the wave functions:

$$\psi_i(x)=A_i e^{ik_i x}+B_i e^{-ik_i x}. \tag{2}$$

The boundary conditions are given by

$$\psi_i(x)=\psi_{i+1}(x), \quad \frac{1}{m_i}\frac{\partial\psi_i}{\partial x}=\frac{1}{m_{i+1}}\frac{\partial\psi_{i+1}}{\partial x}, \tag{3}$$

which determines the coefficient A_i and B_i:

$$\begin{bmatrix}A_{i+1}\\ B_{i+1}\end{bmatrix}=\begin{bmatrix}(1+r_i)e^{ik_i x} & (1-r_i)e^{-ik_i x}\\ (1-r_i)e^{ik_i x} & (1+r_i)e^{-ik_i x}\end{bmatrix}\begin{bmatrix}A_i\\ B_i\end{bmatrix}, \tag{4}$$

where $r_i=(k_i/m_i^*)/(k_{i+1}/m_{i+1}^*)$. Here we assume that the electron is inserted from the channel layer ($i=0$ part), and neglect the reflection amplitude of the wave function of the gate electrode ($B_{N_m}=0$), similar to Ref. [21]. Then the transmission coefficient is given by

$$T_{N_m}(E)\equiv\frac{|k_{N_m}|}{|k_0|}|A_{N_m}|^2. \tag{5}$$

Discrete energy levels of the coupled dots are those when this transmission coefficient has a maximum. We can estimate the effects of the Coulomb interaction of the control qubit on the target qubit shown in Fig. 2. The Coulomb interaction on dot a_1 from dot a_2, and that from the dot b_2, are given by $U_{a_1a_2}=e^2/\epsilon r_{a_1a_2}\rho_{a_2}$ and $U_{a_1b_2}=e^2/\epsilon r_{a_1b_2}\rho_{b_2}$, respectively, where ρ_i is the density of the wave function of dot i, and r_{ij} shows the distance between the center of the dot i and j. We set $\rho_i=0$ or 1 depending on the existence of the localized electron of the neighboring qubits. The Coulomb interaction on the dot b_1 is treated similarly. These Coulomb interactions are added to the potential bottom of the target qubit. For simplicity, we neglect the self-consistent effects.

The localized electron in one of the coupled dots moves into the other dot only if the two discrete energy levels are set to be close (on resonance). The slight change of the relative energy level by the electric field generated by the other set of coupled dots makes impossible the transfer of the localized electron from one dot to the other. The basic concept of this scheme is similar to that of Barenco *et al.* [3]. Whereas Barenco *et al.* used the ground and excited states in a single dot with optical resonant effects, we use only the ground state of the coupled dots with electrical resonant effects (*ground-state operation*). The smaller the size of the dot, the more stable the operation.

Figures 4 and 5 show the calculated results of the controlled-NOT operation in $Si/SiO_2(\epsilon=4)$ material. The barrier height of SiO_2 is assumed to be 3.1 eV, and the effective masses of Si and SiO_2 are assumed to be $0.2m_0$, where m_0 is the mass of a free electron. As the tunneling barrier is sufficiently high, the coupled-dot system can be made smaller in the Si/SiO_2 system than in the $GaAs/Al_xGa_{1-x}As$ system [22]. The diameter of the larger quantum dot is 6 nm, and that of the smaller is 4 nm, where the thickness of the tunneling barrier is 1.5 nm. The distance between centers of the dots of the same size is assumed to be 20 nm (4×10^{12} dots/cm^2). These values are taken from the experiments by Tiwari *et al.* [8]. The thinner the tunneling barrier between the dots in a qubit becomes ($\leqslant$1 nm), the weaker the rate of the localization effect is.

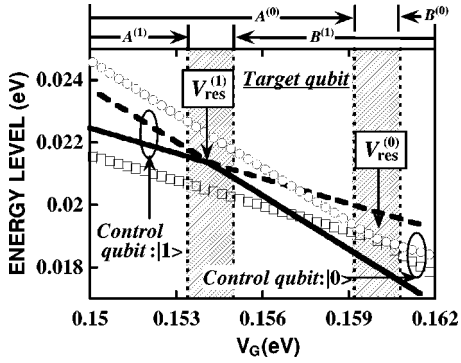

FIG. 4. Relation between the energy levels of electrons of a target qubit and the gate bias for the cases in which the control qubit is in the ''$|1\rangle$'' state ''$|0\rangle$'' states. The structure is channel$|SiO_2$(2.5 nm)$|$Si nanocrystals (6 nm: dot a)$|SiO_2$(1.5 nm)$|$Si nanocrystals (4 nm: dot b)$|SiO_2$(7 nm)$|$gate. $A^{(1)}$ and $B^{(1)}$ show the localized regions in the gate bias for a larger dot (dot a_1 in Fig. 2) and a smaller dot (dot b_1 in Fig. 2), respectively, when the control qubit is in the $|1\rangle$ state. $A^{(0)}$ and $B^{(0)}$ show similar regions when the control qubit is in the $|0\rangle$ state. Hatched areas show the regions of delocalization where the wave functions spread over the two dots. This area shifts depending on whether the control qubit is in the $|1\rangle$ state or $|0\rangle$ state. At the boundaries of these areas, wave functions are delocalized less than 98% in one of the dots, and, at their centers $V_{res}^{(1)}$ or $V_{res}^{(0)}$, wave functions are equally distributed in both dots.

Electron in a target qubit is localized in a larger dot at lower gate bias region (region $A^{(1)}$ in the case where control qubit is in the $|1\rangle$ state in Fig. 4). As the gate voltage is applied, the energy level of the localization in the larger dot exceeds that of the smaller dot. At $V_G = V_{res}^{(1)}$ (the center of the left hatched region in Fig. 4), the wave function of the lowest-energy state (even parity) and that of the excited state (odd parity) spread over the two dots with equal weight, when the control qubit is in the $|1\rangle$ state. The degenerate energy levels of the single dots are split by the coupling of the dots and show the small energy difference ΔE ($\sim 6.28 \times 10^{-5}$ eV, which is not distinguishable in the figure). This resonant gate bias shifts toward the higher-bias region in the case where the control bit is in the $|0\rangle$ state. This is because the electron in the control qubit is localized in a smaller dot and the band bottom of the smaller dot in the target qubit is raised [Fig. 5(b)]. Thus, when we apply the voltage $V_{res}^{(1)}$, in a half-time of an oscillation with time period $\tau_\delta^C \sim \hbar/2\Delta E$ (~ 5.2 ps), the electron moves between alternate dots only if the control qubit is in the $|1\rangle$ state, and we can show the controlled-NOT operation in the coupled-quantum-dot system.

B. Dynamic properties of the qubit of the coupled quantum dots

Note that the wave function shown in Fig. 4 is a static one, and dynamical properties can be easily discussed by solving the time-dependent Schrödinger equation [18] as follows. The localized wave functions in quantum dots a and b, and the eigenenergies, are expressed as $\psi_a(x)$ and $\psi_b(x)$

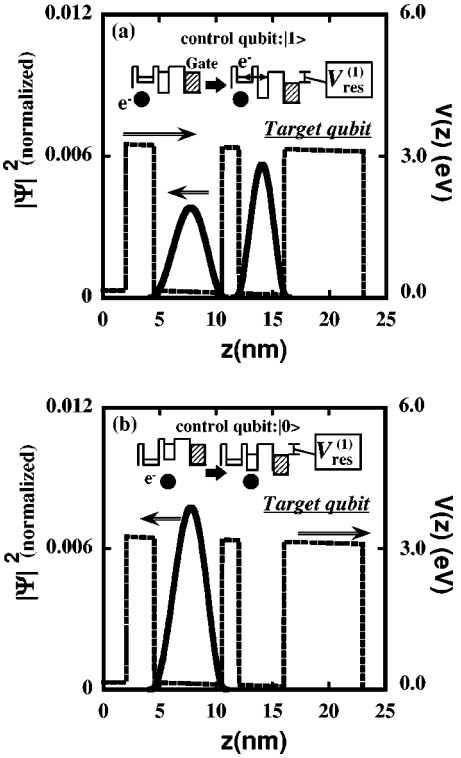

FIG. 5. Spatial dependence of $|\psi|^2$ of the target qubit when the gate bias is $V_{res}^{(1)}$: (a) the control qubit is in the $|1\rangle$ state (the charge of the control qubit is localized in a larger dot near the channel, and the potential of the dot near the channel in target qubit is raised), and (b) the control qubit is in the $|0\rangle$ state (the charge of the control qubit is localized in a smaller dot, and the potential of the smaller dot in target qubit is raised). Wave functions are normalized in the lateral regions of the figures. The amplitude of the normalized wave function refers to the left scale, and the potential profile of the qubit refers to the right scale. This shows the controlled-NOT operation, in which the state of the target qubit is changed in a few picoseconds (dynamical properties) only if the control qubit is in the $|1\rangle$ state.

and, E_a and E_b, respectively, which are assumed to be far apart from each other. Then the coupled wave function is constituted by these wave functions as

$$\psi(x,t) = a(t)\psi_a(x) + b(t)\psi_b(x). \tag{6}$$

The Hamiltonian of the Schrödinger equation, $i\hbar\partial\psi/\partial t = H\psi$, is given by

$$H = -\frac{\hbar^2}{2m}\frac{\partial^2}{\partial x^2} + V_a(x) + V_b(x) - V_0, \tag{7}$$

where $V_0 (= 3.1$ eV) is a barrier height between quantum dots a and b. This equation is easily solved, and the eigenenergies are given as

$$\omega_\pm = (\omega_a + \omega_b)/2 \pm \omega_0, \tag{8}$$

where $\omega_a = E_a/\hbar$, $\omega_b = E_b/\hbar$, $c_a = \langle 1|V_a - V_0|2\rangle/\hbar$, $c_b = \langle 2|V_b - V_0|1\rangle/\hbar$ and $\omega_0 = \sqrt{[(\omega_a - \omega_b)/2]^2 + c_a c_b}$. When

the applied bias sets the energy levels of dots a and b to be the same, and makes the two dots symmetric ($\omega_a=\omega_b$ and $c_a=c_b$),

$$\begin{pmatrix} a(t) \\ b(t) \end{pmatrix} = \begin{pmatrix} \cos(\omega_0 t) & -i\sin(\omega_0 t) \\ -i\sin(\omega_0 t) & \cos(\omega_0 t) \end{pmatrix} \begin{pmatrix} a(0) \\ b(0) \end{pmatrix} e^{-i\omega_a t}. \tag{9}$$

When the time-dependent phase is removed by the interaction picture, this solution shows that it includes the NOT operation in quantum computing, one of the basic single qubit operations. In particular, when the charge is localized in one of the coupled dots in the initial state $[a(0)=1,\ b(0)=0]$, we have

$$a(t)=e^{-i\omega_a t}\cos\omega_0 t, \quad b(t)=-ie^{-i\omega_a t}\sin\omega_0 t. \tag{10}$$

This shows that the localized electron moves completely between dots a and b with a period $\pi/(2\omega_0)$. Thus we can show that the charge transfer is realized when we apply a voltage at which the energy levels of the initially isolated dot coincide, which also corresponds to the case where the energy level of the ground state and that of the excited state of the coupled dots approach one another most closely (hatched area in Fig. 4), in the time period $\pi/(2\omega_0)$. Moreover, in the case of a different initial condition of the charge distribution, $(|0\rangle+|1\rangle)/\sqrt{2}$ is realized as a static state.

Time spent for the transfer of the charge in a coupled quantum dot is given as $\tau_\delta^A=\pi/(2\omega_0)$, with

$$\omega_0=\frac{4}{\hbar}\left(\frac{V_0-E}{V_0}\right)\frac{E}{1+Kl_w}e^{-Kl_d}, \tag{11}$$

where l_w is an average width of the quantum dot (=5 nm), l_d (=1.5 nm) is the width of the tunneling barrier between the two dots, $K=\sqrt{2m(V_0-E)/\hbar^2}$, and E is the energy of the incident electron. We obtained $\tau_\delta^A\sim 12$ ps in the case of Fig. 4, which is longer than the time obtained above (τ_δ^C). This is because this time-dependent approach numerically identifies the exact results when the two dots are far apart [17]. In any event, this numerical mismatch never changes the physical aspects of the coupled-dot system.

Although the speed of the operation becomes faster as the tunneling barrier between the coupled dots in a qubit becomes thinner, the wave function of the qubit of thin tunneling barrier does not localize sufficiently. In the case of our calculation of SiO_2, the criterion of the minimum thickness of the tunneling barrier is considered to be around 1 nm, where the switching speed is estimated to be subpicosecond. Below, the switching speed is also discussed in relation to the measurement time.

III. DISCUSSION

A. Estimation of decoherence time

Here we roughly estimate the decoherence time in a quantum computation of the proposed coupled dots embedded in the SiO_2 material based on the results by Leggett *et al.* [23]. During the quantum computation, the voltage between the source and drain is kept at zero, and there is no flow of the detecting channel current. The decoherence in this case is mainly considered to originate from the phonon environments. SiO_2 is a polar material, and the optical-phonon mode ($\sim$0.153 eV) will be the major dissipation mechanism of the high-temperature, high-energy region. Here we consider the low-temperature region, where only acoustic phonons play a major role in the decoherence mechanism. The effects of this dissipative environment on the two-state system is treated by the infinite bath of harmonic oscillators of acoustic phonons (spin-boson Hamiltonian) where the interaction term between the two-state system and the acoustic phonons is derived from that of amorphous SiO_2 [24,25]. The spectral function $J(\omega)$ is given in the Debye approximation as

$$\frac{1}{2\pi\hbar}J(\omega)=\frac{\gamma^2}{2\pi^2\hbar\rho c^5}\omega^3+\frac{\gamma^2\nu^2}{2\pi^2\hbar\rho c^3 d^2}\omega, \tag{12}$$

where $\gamma\sim 10$ eV, $c\sim 4300$ m/s, $\rho\sim 2200$ kg/m^3, $d\sim 0.5$ nm, and $\nu\sim 10^{-4}$ are the deformation potential, sound velocity, density, lattice constant, and dimensionless parameter, respectively. Here we use the value of the deformation potential of the electrons in the bulk Si, because in the model of Refs. [24,25], the particle in the two-state system is assumed to be an atom. The first term of Eq. (12) is the super-Ohmic part and the second is the Ohmic part. From Ref. [25], the temperature where the Ohmic part appears is estimated to be less than 1 mK.

First we estimate the decoherence time of the super-Ohmic term. Here we treat the case of no bias and denote the bare tunneling frequency as $\Delta\equiv c_a=c_b$. According to Leggett *et al.* [23], the two-state system without bias voltage shows an underdamped *coherent* oscillation, where the damping rate Γ_{so} at $T=0$ is given as

$$\Gamma_{so}=J_{so}(\tilde{\Delta})/4\pi=\frac{\gamma^2\tilde{\Delta}^3}{4\pi\hbar\rho c^5}, \tag{13}$$

where $\tilde{\Delta}$ is the renormalized form of the bare tunneling frequency Δ, defined as

$$\tilde{\Delta}=\Delta\exp\left(-\frac{1}{2\pi\hbar}\int_0^\infty d\omega\frac{J(\omega)}{\omega^2}\right)=\Delta\exp\left(-\frac{\gamma^2\omega_c^2}{2\pi^2\hbar\rho c^5}\right). \tag{14}$$

When we take the above parameters of a-SiO_2 from Ref. [24], and the cutoff $\omega_c=k_B\Theta_D/\hbar$ with $\Theta_D\sim 450$ K, the value of the factor in the exponential is less than -10^3, which extremely reduces the value of $\tilde{\Delta}$ ($\hbar\Delta\sim 10^{-5}$ eV in the above case). The decoherence time derived from the super-Ohmic dissipation, $\tau_{so}=1/\Gamma_{so}$, increases as the $\tilde{\Delta}$ decreases. The direct calculation of the decoherence time becomes more than seconds. This will be because the true microscopic values will be different from those used above, which will be partly the same situation as Ref. [26]. When we use the bare tunneling frequency Δ instead of $\tilde{\Delta}$ in Eq. (13) in order to estimate the shortest decoherence time at the

present, $\tau_{so} \sim 4.8 \times 10^{-7}$ s, during which thousands of quantum calculations can be realized in the proposed system, where the one-step calculation is executed in a few picoseconds. Because $\Delta \ll \omega_c$, this underdamped behavior persists up to a finite temperature (see Leggett *et al.* [23]). However, in order to show the numerical behavior at a finite temperature, we need the microscopic material values which appear in Eq. (14). Thus we cannot show the maximum temperature of operation limited by the above super-Ohmic term here.

At a low temperature region less than 1 mK, Ohmic dissipation should be considered. The dimensionless Ohmic dissipation coefficient $\alpha = \gamma^2 \nu^2/(2\pi^2 \hbar \rho c^3 d^2) \sim 2 \times 10^{-7}$ shows that in our case the *coherent* oscillations survive and the contribution of the incoherent part vanishes in this small-α regime (Ref. [23]).

These ''long'' decoherence times originate from the high potential barrier (SiO_2) between the two coupled quantum dots. By contrast, the short transition time via acoustic phonons in the two-state model of glasses is estimated to be of the order of 10^{-12} s, which is derived from a low barrier height (~ 0.2 eV) and a short distance of the two states (~ 0.1 nm) [27]. These long decoherence times will be related to the ''phonon bottleneck'' of Ref. [28], and effects of phonons are different from those in the bulk [29].

The promising results of the above estimation of the long decoherence time might be due to the simple two-state model of the ideal quantum dots apart from the question of the true microscopic values. When we consider transitions to the excited energy levels in each quantum dot [about 0.018 eV (~ 210 K) above the ground state in the 10-nm Si quantum dot], which will occur at higher temperature regions (>210 K), it is possible that the desirable quantum operation will be limited. Also, as the temperature rises, the effects of optical phonons cannot be neglected, and the decoherence time will be reduced by the energy exchange between the electron and the optical-phonon modes. In particular, when the quantum gate is operated in the ac gate voltage mode of high frequency in a general quantum operation, the dipole of the charge distribution in the coupled quantum dots will be more strongly affected by the electronic environment, and the decoherence time will be reduced. Although there are many problems that need to be investigated in more detail, the above results show that quantum computing in the semiconductor coupled quantum dots seems to be realizable from the viewpoint of one of the elementary steps of the investigation [30].

B. Measurement process

Next, the measurement process of the metal-oxide semiconductor field-effect-transistor (MOSFET) structure is discussed in more detail. We treat the linear region of the channel current, I_d, as $I_d = g_m(V_G - V_{\rm th})$, where g_m is a transconductance of the FET, and $V_{\rm th}$ is a threshold voltage. The change of the charge distribution in the coupled dots induces a shift of the threshold gate voltage $\Delta V_{\rm th}$, which is measured through the variation of the detecting channel current ΔI_d by the field effect. $\Delta V_{\rm th}$ of a single qubit is given approximately by ed_{ab}/ϵ where d_{ab} is the distance between the two dots in a qubit, and found to be of the order of a few tens of meV. This magnitude of the shift of the threshold voltage is found to be of a somewhat smaller order than that reported by Guo *et al.* [9]. The corresponding ΔI_d is given by $\Delta I_d = -g_m \Delta V_{\rm th}$. This measurement process is considered to be similar to that of a quantum point contact (QPC). The measurement process of the coupled dots by QPC has been intensively investigated [31,32]. Here we use the results of Gurvitz [31]. The measurement time $\tau_{\rm ms}$ at the channel current of I_d, can be described as

$$\frac{1}{\tau_{\rm ms}} = \left(\sqrt{\frac{I_d + \Delta I_d}{e}} - \sqrt{\frac{I_d}{e}} \right)^2 . \tag{15}$$

The behavior of the detector can be classified depending on whether $1/\tau_{\rm ms} \ll \Delta$ or $1/\tau_{\rm ms} \gg \Delta$, where Δ is the tunneling frequency of the electron in a qubit. The first case, $1/\tau_{\rm ms} \ll \Delta$, is called a ''weak damping,'' which implies that the electron oscillation in the qubit is faster than the detection, and we will not be able to decide the position of the electron in a qubit. The second case, $1/\tau_{\rm ms} \gg \Delta$, is called a ''strong damping,'' which implies that many electrons can flow through the channel region during an electron oscillation in a qubit. In the latter case, we can induce a ''Zeno time'' $\tau_Z \sim (1/\tau_{\rm ms})/(8\Delta^2)$, and observe the position of the electron in the time interval between $\tau_{\rm ms}$ and τ_Z by the continuous measurements by the Zeno effect.

When we apply these arguments to the experiments of Guo *et al.* [9] at $\Delta V_{\rm th} = 30$ meV, we have $g_m \sim 1.8 \times 10^{-9} \Omega^{-1}$ and $\tau_{\rm ms} \sim 1.7 \times 10^{-6}$ ($\gg 1/\Delta$), if $\hbar\Delta = 10^{-5}$ eV. This shows that the measurement parameters in the results of Ref. [9] are not those of a good detection for $\hbar\Delta = 10^{-5}$ eV. g_m can be simply increased by increasing the bias between the source and drain [8]. These quantum-dot memories are considered to be prototypes, and, in the future, great improvement can be expected, for example, by reducing the resistive parasitics between the source and drain. However, when we would be unable to find a solution capable of improving the speed of transconductance by three orders, it would be necessary to reduce the speed of the gate operation, which can be controlled by the thickness of the tunneling barrier between the coupled dots, so as to realize better detection. In any event, the optimal speed of the gate operation will be able to be increased as the developing fabrication technology improves the measurement speed.

Finally, we consider whether the single-electron transistors (SET) structure proposed by Shnirman and co-workers [33] is more suitable for the measurement than the MOSFET structure. If we adopt the SET structure instead of the MOSFET structure, the Josephson coupling energy E_J of Ref. [33] corresponds to our tunneling matrix element $\hbar\Delta$, and their charging energy term corresponds to our bias term $E_a - E_b$. This is possible because the Hamiltonian of Shnirman and co-workers [33] is described by a two-state system, and their model is considered to be universal in the measurement process in quantum computing. In this case we have to reduce $E_{\rm set}$ to less than that of Shnirman and co-workers in order to suppress the bias term in the coupled dots, and prevent the breakdown of coherence of the two-state system.

Thus the MOSFET structure seems to be available for the read-out device of the semiconductor qubit system, although a strict comparison will be needed. Moreover, problems may be ameliorated as the process technology of conventional LSI advances.

C. Fabrication of the coupled quantum dots

Coupled dots (qubits) can be fabricated by applying the self-limiting oxidation process of a Si nanostructure [34]. For example, the oxidation process after forming Si nanocrystals on a thin amorphous Si layer via a SiO_2 thin film changes the amorphous Si layer and leaves Si dots only under the top Si nanocrystals, which also remain. Thus forming the coupled-dot system is more feasible than controlling donor atoms in substrates. The small fluctuation of the dot sizes is not serious because the on-off gate voltage can be adjusted to be initialized depending on each energy level of each qubit. Another concern is that interface traps may be another localized state and break the coherence of the quantum calculation. However, the density of the trap state ($\sim 10^{10}$ cm^{-2}) is smaller than the assembly of the nanocrystals ($\sim 10^{12}$ cm^{-2}).

IV. CONCLUSIONS

We have proposed a quantum computer based on a coupled-dot system, which can be realized by developing the technology of the single-electron memory with Si nanocrystals. The basic ideas are as follows. (1) The electron is localized in one of the asymmetric coupled dots. (2) Electron transfer takes place from one dot to the other when the energy levels of the coupled dots are set close. (3) The Coulomb interaction between the coupled dots mutually affects the energy levels of the other coupled dots. The estimated decoherence time is found to permit a sufficient number of quantum calculations to be executed. The proposed system, where the direct combination of the quantum circuit and the conventional circuit is possible, is shown to be a promising candidate for the quantum computer.

ACKNOWLEDGMENTS

The author is grateful to K. Sato, N. Gemma, S. Fujita, K. Ichimura, K. Yamamoto, J. Koga, and R. Ohba for fruitful discussions.

[1] A. Ekert and R. Jozsa, Rev. Mod. Phys. **68**, 733 (1996).
[2] N. A. Gershenfeld and I. L. Chaung, Science **275**, 350 (1997).
[3] A. Barenco, D. Deutsch, A. Ekert, and R. Jozsa, Phys. Rev. Lett. **74**, 4083 (1995).
[4] D. Loss and D. P. Divincenzo, Phys. Rev. A **57**, 120 (1998); G. Burkard, D. Loss, and D. P. Divincenzo, Phys. Rev. B **59**, 2070 (1999).
[5] B. E. Kane, Nature (London) **393**, 133 (1998).
[6] A. Shnirman, G. Schön, and Z. Hermon, Phys. Rev. Lett. **79**, 2371 (1997).
[7] Y. Nakamura, Y. A. Pashkin, and J. S. Tsai, Nature (London) **398**, 786 (1999).
[8] S. Tiwari, F. Rana, H. Hanafi, A. Hartstein, E. F. Crabbe, and K. Chan, Appl. Phys. Lett. **68**, 1377 (1996); J. J. Welser, S. Tiwari, S. Rishton, K. Y. Lee, and Y. Lee, IEEE Trans. Electron Devices Lett. **18**, 278 (1997).
[9] L. Guo, E. Leobandung, and S. Y. Chou, Science **275**, 649 (1997).
[10] C. H. Bennett, G. Brassard, C. Crépeau, R. Jozsa, A. Peres, and W. K. Wootters, Phys. Rev. Lett. **70**, 1895 (1993).
[11] C. A. Stafford and S. Das Sarma, Phys. Rev. Lett. **72**, 3590 (1994).
[12] J. Weiss, R. J. Haug, K. v. Klitzing, and K. Ploog, Phys. Rev. Lett. **71**, 4019 (1993).
[13] N.C. van der Vaart, S. F. Godijn, Y. V. Nazarov, C. J. P. M. Harmans, J. E. Mooij, L. W. Molenkamp, and C. T. Foxon, Phys. Rev. Lett. **74**, 4702 (1995).
[14] D. Pfannkuche and S. E. Ulloa, Phys. Rev. Lett. **74**, 1194 (1995).
[15] C. H. Crouch, C. Livermore, R. M. Westervelt, K. L. Campman, and A. C. Gossard, Appl. Phys. Lett. **71**, 817 (1997).
[16] F. R. Waugh, M. J. Berry, D. J. Mar, R. M. Westervelt, K. L. Campman, and A. C. Gossard, Phys. Rev. Lett. **75**, 705 (1995).
[17] A. Yariv, C. Lindsey, and U. Sivan, J. Appl. Phys. **58**, 366 (1985).
[18] N. Tsukada, A. D. Wieck, and K. Ploog, Appl. Phys. Lett. **56**, 2527 (1990).
[19] B. Ricco and M. Y. Azbel, Phys. Rev. B **29**, 1970 (1984).
[20] S. Lloyd, Science **261**, 1569 (1993).
[21] R. Tsu and L. Esaki, Appl. Phys. Lett. **22**, 562 (1973).
[22] R. Tsu, Nature (London) **364**, 19 (1993).
[23] A. J. Leggett, S. Chakravarty, A. T. Dorsey, M. P. A. Fisher, A. Garg, and W. Zwerger, Rev. Mod. Phys. **59**, 1 (1987).
[24] A. J. Garćia and J. Fernández, Phys. Rev. B **55**, 5546 (1997).
[25] A. Würger, Europhys. Lett. **28**, 597 (1994).
[26] H. B. Shore and L. M. Sander, Phys. Rev. B **12**, 1546 (1975).
[27] P. W. Anderson, B. I. Halperin, and C. M. Varma, Philos. Mag. **25**, 1 (1972).
[28] P. Zanardi and F. Rossi, Phys. Rev. Lett. **81**, 4752 (1998).
[29] R. Tsu, Physica B **189**, 235 (1993).
[30] The detailed discussions of the decoherence of this system, e.g., based on the result of L. Viola and S. Lloyd, Phys. Rev. A **58**, 2733 (1998), are beyond the scope of this paper and will appear elsewhere.
[31] S. A. Gurvitz, Phys. Rev. A **56**, 15215 (1997); e-print quant-phys/9806050; e-print quant-phys/9808058.
[32] G. Hackenbroich, B. Rosenow, and H. A. Weidenmüller, Phys. Rev. Lett. **81**, 5896 (1998).
[33] A. Shnirman and G. Schön, Phys. Rev. B **57**, 15400 (1998); G. Schön, A. Shnirman, and Y. Makhlin, e-print cond-mat/9811029.
[34] H. I. Liu, D. K. Biegelsen, F. A. Ponce, N. M. Johnson, and R. F. W. Pease, Appl. Phys. Lett. **64**, 1383 (1994).